MAGNETIC RESONANCE IN MEDICINE 25, 233–247 (1992)

Analysis of Encoding Efficiency in MR Imaging of Velocity Magnitude and Direction

THOMAS E. CONTURO*,† AND BRUCE H. ROBINSON‡

Department of Radiology & Radiological Science, The Johns Hopkins Medical Institutions, Baltimore, Maryland 21205; and ‡Department of Chemistry, University of Washington, Seattle, Washington 98195

Received October 23, 1990; revised June 18, 1991; accepted July 16, 1991

The efficiency of balanced versus unbalanced techniques for phase-angle-based velocity magnitude and direction imaging is investigated. Methods having balanced flow-encoding gradients (gradients in positive and negative directions with a zero center of gravity) are compared with unbalanced methods. For three-dimensional imaging, a currently used balanced method is the six-point technique having opposed gradients pairs for each orthogonal direction. A currently used unbalanced method is a four-point null technique which has three orthogonal gradients and an additional acquisition having no specific flow encoding to correct the baseline (null) phase. In the gradient-limited case of slow flow and perfusion, the balanced method is predicted to have higher velocity magnitude-to-noise ratio per time (SNR_V) by a factor of 1.63, with similar results for velocity direction. In the wraparound-limited case of faster flows and motions, similar results are found when a null acquisition is added to the balanced method. This results in a seven-point balanced method having an SNR_V 1.51 times that of the four-point unbalanced method. If null phases are within the $[-\pi/2, \pi/2]$ interval, this additional null acquisition is unnecessary. Other four-point methods are also considered. These results indicate that, in general, balanced methods have advantages over unbalanced methods for velocity imaging.

INTRODUCTION

In MR vascular imaging, complete flow directional information can be provided, and nonuniformity artifacts caused by vessel tortuosity can be minimized, by obtaining images which are sensitized to flow velocity in orthogonal directions. A flow-sensitized image with direction-independent intensity can then be processed by taking the modulus of the component images. The modulus image has been obtained from velocity components encoded in signal magnitude (*1*) and phase angle (*2, 3*), although phase angle methods can be significantly more efficient in terms of signal-to-noise (*4*). In MR imaging of perfusion (*5, 6*) and tissue (e.g., cardiac) motion (*7*), complex velocity information is also desired. In the present communication the signal-to-noise and time efficiency of different phase-angle-based methods are considered for imaging the velocity magnitude for arbitrary velocity direction. Two separate cases are considered: case A is for high-velocity imaging (e.g., arterial flow and tissue motion) where phase wraparound occurs; case B is for low-velocity imaging (e.g., perfusion) where instrumental

† To whom correspondence should be addressed.

0740-3194/92 $5.00

limits on gradient strength are reached. Optimization of velocity signal-to-noise is important because imaging of slow flow and perfusion is usually limited by noise, even when gradients are full strength, while three-dimensional vascular imaging is usually limited by long acquisition times and low spatial resolution. Signal-to-noise improvement enables a higher dynamic range of velocities to be measured and displayed, and can be exchanged for higher spatial resolution critical for imaging the small vessels detectable in X-ray contrast angiography.

Component velocity-sensitive images can be produced using the phase shifts that occur under the influence of orthogonal bipolar flow-encoding gradients. However, baseline flow-induced phase shifts occur due to factors other than the specific flow-encoding gradients. To make these baseline phase shifts constant for all acquisitions, it is preferred to use a complete pulse sequence repetition for each phase angle acquisition. In this case, the velocity-to-noise ratio depends on the number of acquisitions. Alternatively, phase shifts can be acquired from subsequent echoes in a multiple echo sequence, but echo-to-echo baseline phase changes must be considered (*1*) and, as will be discussed, velocity noise can be adversely affected by T_2 relaxation. Baseline phase shifts have been measured and corrected with a four-point null technique (*2*) using a separate acquisition having no gradient specifically tailored to generate flow information. Then, three additional orthogonally flow-encoding sequences are acquired for full velocity vector imaging. Alternatively, baseline phase shifts have been indirectly taken into account using paired acquisitions having a positive and a negative flow-encoding gradient for each orthogonal direction (*1*) in an octahedral configuration. In this six-point technique, six acquisitions are required for full velocity vector encoding. This six-point technique is called balanced because the combined "weight" of the paired gradients is zero, as will be discussed.

In an analysis of unbalanced methods (*8*), the four-point null method has been shown to be more efficient than an orthogonal six-point method having gradients only in positive directions and having a null acquisition for each flow-encoding direction. The latter acquisition might result when a pulse sequence having a null and flow-encoded acquisition is used to obtain orthogonal velocity components by rotating all logical gradients. In this case, the three null acquisitions are required because baseline flow-induced phase shifts change when all logical gradients are rotated. The following theoretical analysis considers the effect of balancing the six-point method using an octahedral configuration, which is shown to be more efficient than the unbalanced four-point null technique and generally more efficient than other unbalanced four-point techniques.

THEORY AND RESULTS

For determining the x component of velocity, both the six-point-balanced (*1*) and the four-point null (*2*) methods will be considered. In the six-point balanced method, a pair of flow-encoded acquisitions first having a flow-encoding gradient along x and then a flow-encoding gradient along $-x$ result in phase angles ϕ_x and ϕ_{-x}, respectively. Phases are assumed to be reconstructed into the interval $[-\pi, \pi]$ rather than $[0, 2\pi]$ to accommodate phase shifts caused by arbitrary velocity direction. The x component of velocity, V_x, can then be obtained as

$$V_x = \frac{\phi_x - \phi_{-x}}{\gamma \Delta M_{bal}}, \quad [1]$$

where γ is the gyromagnetic ratio and ΔM_{bal} is the change in the first moment of the x flow-encoding gradient between the two balanced acquisitions. In general, the first moment is $\mathbf{M} = \int_0^T \mathbf{G}(t)tdt$, where $\mathbf{G}(t)$ is the gradient vector as a function of time, and the flow-encoding gradient is turned on for time T beginning at $t = 0$. Similar balanced acquisition pairs are obtained sensitized along y and z, and V_y and V_z are obtained by expressions similar to [1].

In the four-point null method, the null phase (ϕ_n) is obtained directly from the reference acquisition having no specific flow-encoding gradient, and velocity sensitivity is produced with three orthogonally flow-encoded acquisitions. The velocity components are obtained as

$$V_x = \frac{\phi_x - \phi_n}{\gamma \Delta M_{nul}}, \quad [2]$$

with analogous expressions for y and z, where ΔM_{nul} is the gradient moment difference between the null and specific flow-encoding gradients.

Equation [2] with analogous expressions for y and z can be rearranged to yield $(\Delta\phi)_{nul} = \gamma \mathbf{V} \cdot \Delta \mathbf{M}_{nul} = \gamma \mathbf{V} \cdot \int_0^T \mathbf{G}tdt$. The resulting phase shift is analogous to the torque produced by the action of gravity (analogous to the flow field) on a uniform linear density ρ_L (analogous to the gradient strength) distributed along the gradient profile. The corresponding torque is $\tau = \mathbf{G}_{grav} \cdot \int_0^T \mathbf{r}dm$, where $\mathbf{r}$ is the distance to the mass element dm. Writing $dm = \rho_L dr$ and imparting the directionality to ρ_L, $\tau = \mathbf{G}_{grav} \cdot \int_0^T \vec{\rho}_L rdr$. Thus, each flow-encoding gradient produces a rotational force or torque which, in the balanced method, is opposed by an opposite gradient producing no net force.

Case A: The Slow Flow or Slow Motion Case (e.g., Perfusion)

For imaging of slow flow and perfusion, velocity determination is often noise-limited and it is particularly important to chose the most optimal technique for noise reduction. In this situation, the gradient moment is determined by instrumental limitations in gradient strength and constraints in gradient duration due to echo time and application of routine imaging gradients. In this case we consider the balanced and unbalanced acquisition schemes with the velocity-encoding gradients at full strength. If the first moment of the positive flow-encoding gradient is m_{max} (the maximum gradient moment for a given echo time TE), then $\Delta M_{bal} = 2m_{max}$ compared to $\Delta M_{nul} = m_{max}$ in the four-point null method (*2*) (see Fig. 1). In this case there will usually be no phase wraparound because resulting phase shifts are small (Fig. 1). The case where there is phase wraparound will be dealt with later.

From Eq. [1], the variance in V_x which is equal to the square of the noise in V_x can then be written in the balanced case as

$$\sigma^2_{bal}(V_x) = \frac{1}{(2\gamma m_{max})^2} [\sigma^2(\phi_x) + \sigma^2(\phi_{-x})]. \quad [3]$$

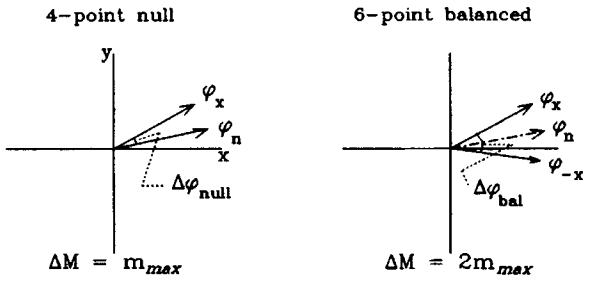

FIG. 1. Typical phase angles in the gradient-limited case such as in slow flow and perfusion. The null phase (ϕ_n) is caused by baseline phase shifts in the absence of flow-encoding gradients. The phase angles after application of the positive and negative flow-encoding gradients are ϕ_x and ϕ_{-x}, respectively. The individual absolute gradient moments are m_{max}, the maximum allowed by the hardware for a given TE interval. The change in gradient moment, ΔM, is thus doubled in the six-point balanced method.

The phase angle noise, given by the standard deviation $\sigma(\phi)$, is equal to the noise-to-signal ratio of the corresponding magnitude-reconstructed signal-intensity image (*4*), and therefore $\sigma(\phi)$ is independent of the actual phase angle. Specifically, $\sigma(\phi) = \sigma(|I|)/|I| = \mathrm{SNR}_I^{-1}$ (*4*), where $|I|$ is the signal intensity obtained by magnitude reconstruction of the raw data used for phase angle determination, and SNR_I is the signal-to-noise ratio in the magnitude-reconstructed image ($\mathrm{SNR}_I > 2$ is assumed). Phase angle dynamic range is defined as the phase angle range divided by the minimal discriminable phase (i.e., the phase noise). Thus, the phase angle dynamic range is a factor 2π that of signal magnitude (*4*) since phase angles are reconstructed over the $[-\pi, \pi]$ interval. Because phase angle noise is dependent on signal magnitude, the two phase angle variances in Eq. [2] will be equal only if the corresponding signal magnitudes are equal. Such will be the case if the pulse sequence is properly designed so that the flow-encoding gradients cause no significant signal intensity loss (and add no additional noise), whereupon $\sigma(\phi_x) = \sigma(\phi_{-x}) = \sigma(\phi_0)$ with $\sigma(\phi_0)$ being the inherent phase angle noise. Equation [3] then becomes

$$\sigma^2_{\mathrm{bal}}(V_x) = \frac{2}{(2\gamma m_{\mathrm{max}})^2}\,\sigma^2(\phi_0) \qquad [4a]$$

$$= \frac{2}{(2\gamma m_{\mathrm{max}}\,\mathrm{SNR}_I)^2}\,. \qquad [4b]$$

Thus, the velocity component noise is independent of the actual component velocity and is only dependent on gradient moment and inherent signal detection sensitivity (expressed as SNR_I). Identical equations hold for V_y and V_z. Equations [1] and [4b] will be used to determine the velocity signal-to-noise and the minimum detectable velocity component for a given pulse sequence.

Similarly, for the four-point null method in the gradient-limited case, Eq. [2] yields

$$\sigma^2_{\mathrm{nul}}(V_x) = \frac{1}{(\gamma m_{\mathrm{max}})^2}\,[\sigma^2(\phi_x) + \sigma^2(\phi_n)] \qquad [5a]$$

$$= \frac{2}{(\gamma m_{\mathrm{max}}\,\mathrm{SNR}_I)^2}\,. \qquad [5b]$$

Comparing Eqs. [4b] and [5b] shows that the noise in the null method is twice that of the balanced method for one-component imaging of slow velocities.

Velocity Magnitude

In the case of arbitrary velocity directions, the velocity magnitude $\|\mathbf{V}\| = V$ is calculated as

$$V = \sqrt{V_x^2 + V_y^2 + V_z^2}. \quad [6]$$

In the six-point balanced method, the errors in the component velocities are uncorrelated because each component is determined by an independent pair of measurements. Moreover, if the signal magnitudes of the different acquisitions are equal, these component velocity errors are given by equations analogous to [4a] so that $\sigma(V_x) = \sigma(V_y) = \sigma(V_z) = \sigma(V_0)$, where $\sigma(V_0)$ is the inherent velocity component noise. From [6], the noise in velocity magnitude using the balanced method is then

$$\sigma_{\text{bal}}(V) = \sigma_{\text{bal}}(V_0). \quad [7]$$

In the unbalanced four-point null method, velocity magnitude again is obtained according to Eq. [6]. Unlike the balanced method, however, the noise in the velocity components is correlated because the same null phase is used to correct the phase of each component, as discussed by Pelc and Bernstein (*8*). In the two-dimensional case, the variance in velocity magnitude is given by

$$\sigma^2(V) = \left(\frac{\partial V}{\partial V_x}\right)^2 \sigma^2(V_x) + \left(\frac{\partial V}{\partial V_y}\right)^2 \sigma^2(V_y) + 2\rho_{xy}\left(\frac{\partial V}{\partial V_x}\right)\left(\frac{\partial V}{\partial V_y}\right) \sigma(V_x)\sigma(V_y), \quad [8]$$

where ρ_{xy} is the coefficient of correlation between the noise in V_x and V_y. In the three-dimensional case, there are three correlation coefficient terms and six overall terms in Eq. [8]. The values of the correlation coefficients are not obvious, but they can all be determined to be 0.5 by analyzing noise with basic principles as in the Appendix. The result is (see Appendix)

$$\sigma_{\text{nul}}^2(V) = \frac{\sigma_{\text{nul}}^2(V_0)}{2}\left[1 + \frac{(V_x + V_y + V_z)^2}{V^2}\right], \quad [9]$$

which agrees with results of Pelc and Bernstein (*8*). As discussed (*8*), the noise is direction-dependent, and the mean value of $f = (V_x + V_y + V_z)^2/V^2$ averaged over all three-dimensional directions is 1. The actual value of $f = 1$ is obtained when the velocity vector is directed along any of the principle cartesian axes. In the two-dimensional case, $\sigma_{\text{null}}(V)$ ranges from 0.71 to 1.2 times $\sigma_{\text{null}}(V_0)$ whereas, in the three-dimensional case, $\sigma_{\text{null}}(V)$ ranges from 0.71 to 1.4 times $\sigma_{\text{null}}(V_x)$. The correlation of noise among the velocity components produces this direction dependence without changing the mean noise. From Eq. [5b], the mean noise in velocity magnitude using the null method is then

$$\langle \sigma_{\text{nul}}(V) \rangle \approx \sigma_{\text{nul}}(V_0). \quad [10]$$

This expression is only approximate because $\langle \sigma_{\text{nul}}^2(V) \rangle \neq \langle \sigma_{\text{nul}}(V) \rangle^2$. However,

the approximation in Eq. [10] is valid because the variation in $\sigma_{nul}(V)$ with direction is small.

Combining Eqs. [4], [5], [7], and [10], the velocity noise in the balanced method is shown to be half that of the four-point null method in the slow flow/motion case. As the null method requires only four acquisitions compared to the six acquisitions of the balanced method, the former method can be signal-averaged relative to the latter, thereby improving signal-to-noise proportional to the square root of the acquisition time. Therefore, in the three-dimensional case with slow flow/motion, the balanced method is more efficient in terms of the velocity-to-noise ratio per unit scan time (SNR_V) by a factor of $2\sqrt{4/6} \approx 1.63$ (Table 1). The six-point method having three null acquisitions (*8*) has a relative SNR_V of $\sqrt{4/6} = 0.81$.

Case B: The Fast Flow or Fast Motion Case (e.g., Arterial Flow)

In the case of fast arterial flow or fast tissue motion, the choice of gradient moment is usually limited by phase wraparound. The technique that is more efficient depends on the magnitude of the null phase and the phase angle reconstruction technique. Null phase shifts have both a static component (field inhomogeneities, field frequency mismatch, magnetic susceptibility, echo time centering, etc.) and a motion-induced component (flow along imaging gradients, RF propagation through tissues (*9*), etc.). Phase shifts due to static effects can be minimized by sequence tuning and by zero- and first-order phase correction at reconstruction time [e.g., see (*4*)]. Phase shifts due to flow effects can be reduced by using slice-selecting and readout gradients which are flow-compensated [i.e., have a first moment equal to zero (*10*)].

The larger the null phase, the more readily the wraparound phase will be reached when flow-encoding is turned on (Fig. 2a). If the null phase extends from $[-\pi, \pi]$ throughout the image, absolute phase angles greater than π could even result from small gradient moments (Fig. 2a). Because the direction of flow is usually not known a priori in three-dimensional applications, then the gradient strength that induces a wraparound in the six-point balanced method will be the same as that necessary to induce wraparound in the four-point balanced method (cf., Figs 2a and 2b); this common gradient moment is given by the expression in Fig. 2. Therefore, in the high-velocity case with direct reconstruction of individual phase angles, Eqs. [4]–[5] are valid with m_{max} replaced by the gradient moment expressions in Fig. 2, so that the relative velocity-to-noise ratio (SNR_V) of the two methods is the same as in the slow flow case.

In the fast flow case where individual phase angle images contain regions of phase wraparound (Figs. 2a and 2b), wraparound in the resulting velocity image can potentially be reduced in the four-point null case by direct reconstruction of the phase angle difference by complex division (*11*). The phase difference can be calculated as $(\Delta\phi)_{null} = \phi_x - \phi_n = \arg(Z_x/Z_n)$, where Z represents a complex signal. The complex ratio expresses the numerator with the real axis of the complex coordinate system rotated onto the denominator. Thus, this operation effectively rotates the null phase in Fig. 2a to zero and equally rotates the x-encoded phase on a pixel-by-pixel basis analogous to a regional adjustment done previously (*4*). Without changing noise, the complex ratio operation can effectively "down-convert" large individual phase angles into one smaller phase value $\Delta\phi = \phi_x - \phi_n$ which will not wrap as long

TABLE 1

Comparative Efficiencies of Unbalanced Four-Point and Balanced Six-Point Methods

Pulse method	$\sigma^2(\|V\|)$[a]	Number of acquisitions (N_{aq}) 3D	2D	1D	Relative[b] SNR_V 3D	2D	1D	3D time reduction factor[c]
		Gradient-limited						
Four-point null[d]	$2/1k \propto 2$	4	3	2	1.0	1.0	1.0	1.0
Four-point isosensitive[e]	$4/2^2k \propto 1$	4	4	4	1.41	1.22	1.0	2.0
Six-point balanced[f]	$2/2k \propto 0.5$	6	4	2	1.63	1.73	2.0	2.67
Four-point nonzero ref[g]	$2/2^2k \propto 0.5$	4	3	2	2.0	2.0	2.0	4.0

Pulse method	$\|\Delta\phi\|$[i]	Number of acquisitions 3D	2D	1D	Absolute[h] SNR_V/SNR_I (relative[b] SNR_V) 3D	2D	1D	3D time reduction factor[c]
		Wraparound-limited						
Four-point null[d]	π	4	3	2	1.11	1.28	1.57	1.0
Six-point balanced with $\|\phi_n\| < \pi/2$[f]	2π	6	4	2	1.81 (1.63)	2.22 (1.73)	3.14 (2.0)	2.67
Seven-point balanced with ϕ_n acquisition	2π	7	5	3	1.68 (1.51)	1.99 (1.55)	2.57 (1.63)	2.29

[a] The numerator represents the phase angle combinations and the denominator represents the change in gradient moment. The constant $k = (\gamma m_{max}\, SNR_I)^{-1}$.

[b] Signal-to-noise ratio of velocity magnitude corrected for acquisition time and relative to the unbalanced 4-point null method. Results are also valid for imaging of directional angle.

[c] Factor by which the imaging time is reduced relative to the 4-point null method for three-directional velocity imaging at an equivalent noise level. Imaging time is proportional to $\sigma^2(|V|) \times (N_{aq})$.

[d] Variance is direction-dependent and is averaged over all directions.

[e] Four-point isotropically sensitive method. The analysis in the wraparound-limited case is more complicated and will not be considered here.

[f] Identical results are found for the ideal case in which the velocity component can be obtained directly from a single phase angle acquisition (i.e., if the null phase is always zero).

[g] Method having four gradients along $(\bar{1}, \bar{1}, \bar{1})$, $(1, \bar{1}, \bar{1})$, $(\bar{1}, 1, \bar{1})$, and $(\bar{1}, \bar{1}, 1)$ as described in the text. In the wraparound-limited case, this reduces to the 4-point null method.

[h] Velocity-to-noise ratio relative to the intensity-to-noise ratio of signal magnitude, and calculated from $SNR_V = |\Delta\phi|/(\sqrt{2}\sqrt{N_{aq}})$ as described in the text below Eq. [13].

[i] The $|\Delta\phi|$ that would result from rotating the peak velocity vector onto the velocity-encoded axis.

as $|\phi_x - \phi_n| < \pi$. Others also assume that the magnitude of paired phase angle differences must be kept less than or equal to π (*12*). Therefore, using complex division, the gradient moment in the unbalanced four-point null method can be increased to m_π (Fig. 2c), where m_π is the moment that produces an absolute incremental phase shift of π for the given maximal velocity of interest. When $|\phi_x - \phi_n|$ does exceed π, wraparound can then be corrected on a regional basis as

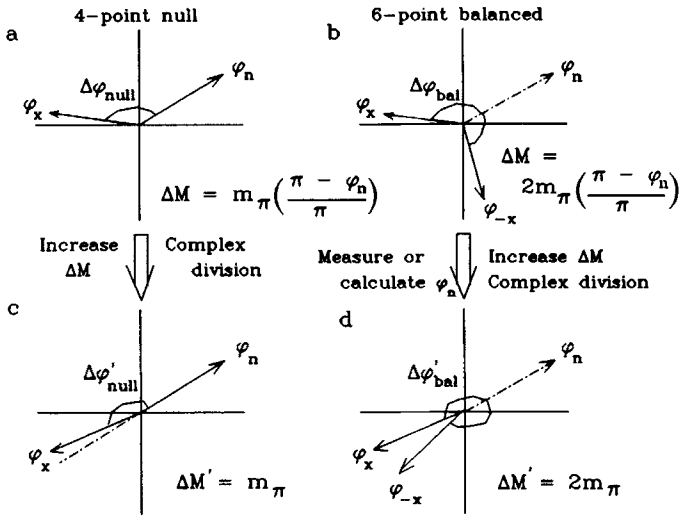

FIG. 2. Typical phase angles in the wraparound-limited case such as in fast flow and tissue motion. If individual phase angles are reconstructed directly, the gradient moment must be lowered by the same amount in both four-point null (a) and balanced (b) methods because the velocity direction is not known. The moment is lowered according to the given expression, where m_π is the gradient moment that causes the absolute phase to be incremented by π. If complex division of the raw data is available, the gradient moment can be increased to m_π in the four-point null case as now only the phase difference must be within $[-\pi, \pi]$. In the balanced case (d), the individual gradient moments can also be increased to m_π if the null phase is acquired. Alternatively, the null phase can be calculated in (d) from the average of ϕ_x and ϕ_{-x}, also enabling the gradient moment to be increased to m_π. However, the calculated ϕ_n is only correct if ϕ_n is in the $[-\pi/2, \pi/2]$ interval (see text).

described (*4*). A similar reconstruction of the six-point balanced method would require the individual gradient moments to be halved to $m_\pi/2$ so that $\Delta M = m_\pi$ as in the four-point null method. However, if the null phase can be determined, the individual gradient moments in the balanced method can be restored to the optimal value of m_π (Fig. 2d) because the differences $\phi_x - \phi_n$ and $\phi_{-x} - \phi_n$ both will be in the $[-\pi, \pi]$ interval. The null phase will be the mean value of ϕ_x and ϕ_{-x} and can be calculated as $\phi_n = \arg(Z_n)$ where $Z_n = (Z_{-x} \cdot Z_x)^{1/2}$. This calculation is unambiguous and correct when $|\phi_n| < \pi/2$ (Fig. 2d), as verified by computer simulation. Thus, if the acquisition and reconstruction can be tuned so that the null phase is small throughout the region of interest [see, e.g. (*4*)], the total phase shift can be accurately calculated as $\Delta\phi_{bal} = \arg(Z_x/Z_n) + \arg(Z_n/Z_{-x})$. The two arguments will be either both positive or both negative. When both are positive, results are defined over $[0, 2\pi]$. When both are negative, results are defined over $[-2\pi, 0]$. Therefore, by calculating the null phase, $\Delta\phi_{bal}$ is principle-valued over $[-2\pi, 2\pi]$ as verified by computer simulation. The terms on the right-hand side of the above equation for $\Delta\phi_{bal}$ appear to depend on the noise of ϕ_n, but in fact do not. In this situation, $\Delta M_{bal} = 2m_\pi$ compared to $\Delta M_{nul} = m_\pi$, and the balanced method will have half the noise and an SNR_V of $2\sqrt{4/6} \approx 1.63$ relative to the four-point null method (Table 1).

Seven-Point Balanced Method in the High-Velocity Case

By a similar argument, in the wraparound-limited case with completely arbitrary ϕ_n, the individual gradient moments of the balanced acquisition can be restored to m_π if ϕ_n is directly measured (Fig. 2d). In fact, as discussed above, all that needs to be determined is whether or not $|\phi_n| \leq \pi/2$. If the balanced method is used with an additional null acquisition (a seven-point balanced method), the velocity component can be determined as

$$V_x = \frac{(\phi_x - \phi_n) - (\phi_{-x} - \phi_n)}{2\gamma m_\pi} = \frac{\Delta\phi_{bal}}{2\gamma m_\pi}, \qquad [11]$$

where each phase difference in the parentheses in [11] is principle-valued in the $[-\pi, \pi]$ interval. The additional null acquisition is merely for orientation (e.g., the measured null need only differentiate between a correctly calculated null vector Z_n in Fig. 2d and a Z_n which points in the opposite direction). Thus, the null acquisition does not add noise, as verified by the cancellation of ϕ_n in Eq. [11] and by an analysis of the correlated noise in [11] similar to that in the Appendix. This cancellation does not occur when using multiple null phases as in the six-point method having three null acquisitions (*8*). In the seven-point balanced method, the net phase shift is then determined as $\Delta\phi_{bal} = \arg(Z_x/Z_n) - \arg(Z_{-x}/Z_n)$, which is principle-valued in the $[-2\pi, 2\pi]$ interval. The noise of the balanced method has been restored to half that of the four-point null method with only one additional acquisition so that the relative SNR_V is $2\sqrt{4/7} \approx 1.51$ (Table 1). In the cases of two- and one-component velocity imaging such as might be done when imaging flow in the sagittal sinus or spine, respectively, the SNR_V is also given in Table 1. It is noteworthy that, in comparing the seven-point balanced and four-point null methods, the beneficial effect of doubling the gradient moment easily offsets the adverse effect of increasing the number of acquisitions.

Incidentally, phase wraparound can also occur in the slow flow, gradient-limited situation (see case A and Fig. 1) in the rare instance that the null phase (ϕ_n) is very close to $\pm\pi$. However, as in the wraparound-limited case (case B), wraparound in the final velocity image can be eliminated by complex division.

Other Unbalanced Four-Point Methods

Other four-point methods which are unbalanced have been introduced and will be considered here. The novel four-point null method developed by Pelc and Bernstein (*8*) having gradients bisecting the cartesian axes has isotropic sensitivity. Using an expression given elsewhere (*8*), the gradient-limited SNR_V of the isotropically sensitive method is only $\sqrt{2}\sqrt{4/4} = 1.41$ times that of the four-point null method (Table 1) compared to a relative SNR_V of 1.63 for the balanced six-point method. In the wraparound-limited case, the comparison is more complicated and will be considered later (*13*). A four-point method having a nonzero phase reference can be devised. For example, the reference phase acquisition can have a gradient aligned along $(\bar{1}, \bar{1}, \bar{1})$, followed by gradients along $(1, \bar{1}, \bar{1})$, $(\bar{1}, 1, \bar{1})$, and $(\bar{1}, \bar{1}, 1)$. This arrangement is more centered around the origin than the four-point null method and can thus be considered semi-balanced. Because gradients span plus and minus directions, the change in gradient moment is $2m_{max}$ in the gradient-limited case, identical to the six-

point balanced method. The method then is more efficient than the six-point balanced method by a factor of $\sqrt{6/4} = 1.22$ (Table 1). However, in this nonzero reference method, noise is direction-dependent. Moreover, in the wraparound-limited high-velocity case, gradient moments cannot be "bridged" by a null acquisition since the gradients are not balanced. In this case, gradients must be reduced in half relative to the balanced method. The nonzero phase reference method will also be discussed in more detail later (*13*).

Absolute SNR_V and SNR_I Analysis

The SNR_V can be placed on an absolute scale for computation of actual velocity sensitivity and for comparison with signal magnitude methods. The dynamic range in the V_x image (DR_{V_x}) is obtained using Eqs. [1] and [4] as

$$DR_{V_x} = \frac{\text{Range in } V_x}{V_x \text{ Noise}} \qquad [12a]$$

$$= \frac{\text{Range in } \Delta\phi_{\text{bal}}}{\sqrt{2}} SNR_I. \qquad [12b]$$

The SNR_I in Eq. [12] is for a single acquisition, whereas the V_x measurement having the given dynamic range requires two acquisitions. Therefore, to compare DR_{V_x} and SNR_I on an absolute scale, DR_{V_x} is divided by the square root of the number of acquisitions. For the high-velocity one-component balanced case with $\Delta M = 2m_\pi$ and with the velocity directed along x, $\Delta\phi$ in [12b] ranges from $[-2\pi, 2\pi]$. Thus, the dynamic range in the V_x image is $4\pi/(\sqrt{2}\sqrt{2})\ SNR_I = 2\pi\ SNR_I \approx 6.28\ SNR_I$, which is identical to the dynamic range in a single phase angle image (*4*).

From Eq. [4], the noise in velocity magnitude, $\sigma(V)$, is independent of velocity direction. Therefore, any arbitrary velocity vector can be rotated onto the x axis so that $V = |V_x|$. Then the velocity-to-noise ratio, SNR_V, is obtained from Eq. [4] and from the absolute value of Eq. [1] as

$$SNR_V = \frac{V}{\sigma(V)} = \frac{|\Delta\phi_{\text{bal}}|}{\sqrt{2}} SNR_I. \qquad [13]$$

Thus, the SNR_V is half the dynamic range of an individual velocity component. Specifically, in the seven-point balanced method, $\Delta\phi$ is principle-valued over $[-2\pi, 2\pi]$ so that $SNR_V = 2\pi/\sqrt{2}\sqrt{7})\ SNR_I = 1.68\ SNR_I$ accounting for the number of acquisitions. In general, the maximum SNR_V is half the range in phase angles divided by the square root of the number of phase angles used for each component velocity calculation (only phase angles that contribute noise are counted), and further divided by the square root of the total number of acquisitions. The absolute SNR_V for other methods is summarized in Table 1.

The high SNR_V/SNR_I ratios in Table 1 emphasize that velocity imaging methods based on phase angle reconstruction can be much less noisy than methods based on signal magnitude reconstruction (*4*). For example, the SNR_V/SNR_I ratios represent the signal-to-noise in a vessel imaged by the phase angle method relative to, e.g., imaging the vessel by magnitude reconstruction with suppression of static signals.

It is interesting that the SNR_V of the six-point balanced method with $|\phi_n| < \pi/2$ is equal to that of the ideal case where all three velocity components can be obtained with the minimum three acquisitions (i.e., null phases are zero). In this ideal case with the velocity vector rotated onto the x axis, there is a 1:1 correspondence between V_x and ϕ_x so that $[-V_x, V_x]$ maps onto $[-\pi, \pi]$. Therefore, $SNR_V = (\pi/\sqrt{3})\ SNR_I \approx 1.81\ SNR_I$ equal to the SNR_V for the six-point balanced method (Table 1). The six-point balanced method thus does not merely correct the null phase, but also restores SNR_V to the ideal case.

DISCUSSION

The velocity-to-noise efficiency of different gradient schemes in current use have been analyzed. In general, it can be concluded that truly geometrically-balanced methods have significant advantages over unbalanced methods in that (1) gradient strengths span positive and negative values resulting in higher SNR_V; (2) the null phase need not be measured in the low-velocity case, avoiding unnecessary noise; (3) the null phase can be used in the high-velocity case to extend phase angle ranges and SNR_V for velocity in all directions; and (4) velocity noise will be direction-independent. In the isotropically sensitive four-point method (*8*) which is not fully balanced, only the fourth advantage is achieved. The semi-balanced nonzero reference method has only the first two features. These conclusions have provided the motivation for development of tetrahedral gradient schemes which are even more optimal (*13, 14*).

The assumptions in this analysis are that the signal-to-noise ratio in intensity magnitude (SNR_I) is equal in the different acquisitions and different techniques. Similarly, the velocity-encoding gradient magnitude is assumed to be known and equal in the different acquisitions and techniques. In the high-velocity case, an additional assumption is that the maximum velocity is known so that the gradient moment m_π can be selected to cause phase shifts just below the threshold for wraparound. The SNR_I assumption will be valid if the pulse sequence and flow compensating gradients are optimally designed, and if the dephasing caused by flow-encoding gradients (due to intravoxel velocity gradients) is negligible. Such dephasing will be minimized by using high-resolution techniques made possible by the SNR_V improvements discussed. If phases are obtained from a multiple spin-echo sequence (*1*), intensities will not be constant and velocity noise may have significant direction dependence.

The presented velocity-to-noise analysis is based on phase angle measurements. However, if the magnitude of the complex signal difference $|\Delta Z| = |Z_x - Z_n|$ is used for contrast (*15, 16*), there is a similar benefit in using balanced gradient methods because, in the case of small phase shifts $\Delta\phi$, $\Delta\phi \approx \sin(\phi) \approx \tan(\phi)$ and $|\Delta Z| \approx |Z_x| \cdot \Delta\phi$. Moreover, if velocity direction, Θ_V, is obtained as, e.g., $\Theta_V = \tan^{-1}(V_y/V_x)$, then $\sigma(\Theta_V) = \sigma(V)/V$ by an analysis similar to that of phase angle noise (*4*). Therefore, the balanced method is also advantageous for velocity direction imaging according to Table 1.

As mentioned after Eq. [2], measuring the phase shift caused by the interaction of magnetic gradients and velocity fields is analogous to measuring the torque caused by the interaction of density distributions and gravitational fields (e.g., measuring the deflection caused by an unknown weight placed on a double-beam balance). In the

former case, the gradients are known and the velocity is calculated whereas, in the latter, the gravitational field is known and the mass is to be calculated.

In a classic article, Hotelling considered several schemes for weighing with a double-beam balance (*17*), the most analogous being the weighing of two objects after the balance has been tared. He showed that, instead of weighing two objects a and b individually, it is more precise to first weigh the objects together on the same pan, second weigh the difference by placing the two objects on different pans, and then third subtract the two readings. In a one-dimensional velocity measurement, the weight of a can be considered to be the null phase ϕ_n, and the weight b the additional specific phase $\Delta\phi$ due to the flow-encoding gradient, where b is to be determined. Weighing the sum and the difference is entirely analogous to the balanced method (case A), whereas weighing $a + b$ (i.e., ϕ_x) and then subtracting a is analogous to the null method (case B), which is even less precise than Hotelling's case of measuring b individually.

To analyze the seven-point balanced method in one dimension, consider weighing an object ϕ_x in one pan, then the same object in the other pan (ϕ_{-x}), and then measuring the tare (ϕ_n) without any weights. To compare the four-point null method, three weighings are also allowed: The object ϕ_x is weighted twice in the same pan, and then the tare (ϕ_n) is measured. By an analysis similar to Hotelling's, it can be shown that the object's variance in the balanced case is one-third of that if the unbalanced case. Therefore, the negative weighting or negative gradient acquisition in the balanced method improves precision much more than by a mere averaging of the positive acquisition.

CONCLUSION

In flow and perfusion imaging it is useful to accurately determine velocity magnitude and direction, for example, to minimize directional artifacts in curved and tortuous vessels. It has previously been shown that methods based on phase angle reconstruction are more efficient in terms of signal-to-noise per time than those based on magnitude reconstruction. In this work the efficiency of phase-angle-based velocity magnitude imaging is theoretically determined. Currently used methods for correcting the flow-induced phase shifts that occur in the absence of specific flow-encoding gradients are considered. The four-point null method uses a single additional acquisition having no specific flow encoding to directly measure the baseline (null) phase. The six-point balanced method uses acquisition pairs having opposed flow-encoding gradients for each orthogonal component to indirectly account for the baseline phase. In the slow velocity case, the balanced method is theoretically predicted to be more efficient in terms of velocity-to-noise ratio by approximate factors of 1.63, 1.73, and 2.0 for three-, two-, and one-component velocity imaging, respectively. Reduction in the total scan time needed to obtain a given velocity-to-noise ratio can be as large as a factor of 4 despite the greater number of acquisitions in the balanced method. A semi-balanced method having a nonzero phase reference has even higher velocity-to-noise in the slow flow case, but also has direction-dependent noise. In the fast velocity case, similar results can be obtained with complex algebraic manipulations when the null phase is known to be restricted to the $[-\pi/2, \pi/2]$ interval. If the null phase is unrestricted, the balanced method can be used with an additional null acquisition, resulting in a

velocity-to-noise ratio 1.51 times that of the four-point null or nonzero reference methods. The four-point isotropically sensitive method is less efficient than the balanced method in all cases. In general, true geometrically balanced methods such as the six-point octahedral method have significant advantages.

APPENDIX

The noise in the velocity magnitude in Eq. [6] is desired. For multiple measurements of V, each has a deviation from the true V given by

$$\epsilon_i = \bar{V} - V_i, \qquad [1A]$$

where V_i is a single measured velocity magnitude and $\bar{V}$ is the average velocity magnitude. The variance in V is then given as

$$\sigma^2(V) = \frac{\sum_{i=1}^{N} \epsilon_i^2}{N}, \qquad [2A]$$

where N is the number of measurements. From Eq. [5b], the noise levels in V_x, V_y, and V_z are known so it is desired to express Eq. [1A] in terms of the deviations in V_x, V_y, and V_z. This cannot directly be done by substituting Eq. [6] into Eq. [1A] because of the nonlinearity of Eq. [6]. However, [6] can be linearized in terms of V_x, V_y, and V_z by expanding V_i about the known average, $\bar{V}$, in a Taylor series:

$$V_i = \bar{V} + (V_{x_i} - \bar{V}_x)\frac{\bar{V}_x}{V} + (V_{y_i} - \bar{V}_y)\frac{\bar{V}_y}{V} + (V_{z_i} - \bar{V}_z)\frac{\bar{V}_z}{V} + \cdots. \qquad [3A]$$

For small noise fluctuations, higher order terms can be neglected, and substitution of Eq. [1A] into Eq. [3A] yields

$$\epsilon_i = \epsilon(V_x)_i R_x + \epsilon(V_y)_i R_y + \epsilon(V_z)_i R_z, \qquad [4A]$$

where $\epsilon(V_x)_i = V_{x_i} - \bar{V}_x$ and $R_x = \bar{V}_x/\bar{V}$, with similar expressions for y and z. Now the variance defined by Eq. [2A] can be written in terms of the variance in the velocity components. However, the latter are correlated in Eq. [2] due to the common null phase. Therefore, Eq. [4A] must be written in terms of the uncorrelated phase angle fluctuations by writing the deviations in Eq. [2] as

$$\epsilon(V_x)_i = k(\epsilon_{x_i} - \epsilon_{n_i}), \qquad [5A]$$

where $k = (\gamma \Delta M)^{-1}$ and ϵ_{x_i} is a noise fluctuation in ϕ_x, with similar equations for y and z. Substituting [5A] into [4A] and then substituting [4A] into [1A], the variance in V defined in Eq. [2A] becomes

$$\sigma^2(V) = \frac{k^2}{N}\sum_{i=1}^{N}(\epsilon_{x_i}R_x - \epsilon_{n_i}R_x + \epsilon_{y_i}R_y - \epsilon_{n_i}R_y + \epsilon_{z_i}R_z - \epsilon_{n_i}R_z)^2. \qquad [6A]$$

The cross-product terms in Eq. [6A] are zero since errors are normally distributed about the mean, yielding the expression

$$\sigma^2(V) = \frac{k^2}{N}\sum_{i=1}^{N}[\epsilon_{x_i}^2 R_x^2 + \epsilon_{y_i}^2 R_y^2 + \epsilon_{z_i}^2 R_z^2 + \epsilon_{n_i}^2(R_x^2 + R_y^2 + R_z^2 + 2R_xR_y + 2R_xR_z + 2R_yR_z)]. \quad [7A]$$

Using the definition of phase noise as $\sigma^2(\phi_x) = \sum_i \epsilon_{x_i}/N$ and similar expressions for ϕ_y, ϕ_z, and ϕ_n, Eq. [7A] becomes

$$\sigma^2(V) = k^2\{[\sigma^2(\phi_x) + \sigma^2(\phi_n)]R_x^2 + [\sigma^2(\phi_y) + \sigma^2(\phi_n)]R_y^2 + [\sigma^2(\phi_z) + \sigma^2(\phi_n)]R_z^2 + 2\sigma^2(\phi_n)(R_xR_y + R_xR_z + R_yR_z)\}. \quad [8A]$$

From Eq. [2] and the definition of k, $\sigma^2(V_x) = k[\sigma^2(\phi_x) + \sigma^2(\phi_n)]$, so that Eq. [8A] becomes

$$\sigma^2(V) = R_x^2\sigma^2(V_x) + R_y^2\sigma^2(V_y) + R_z^2\sigma^2(V_z) + 2(R_xR_y + R_xR_z + R_yR_z)[k\sigma(\phi_n)]^2. \quad [9A]$$

Writing $\sigma(V_x) = \sigma(V_y) = \sigma(V_z) = \sigma(V_0)$ as discussed, and expanding the ratios R, Eq. [9A] becomes

$$\sigma^2(V) = \sigma^2(V_0) + 2\left(\frac{V_xV_y + V_xV_z + V_yV_z}{V^2}\right)[k\sigma(\phi_n)]^2. \quad [10A]$$

If the null and x-encoded intensity magnitudes are the same, $\sigma^2(V_0) = \sigma^2(V_x) = 2k\sigma^2(\phi_n)$ using the expression below Eq. [8A]. Equation [10A] then becomes

$$\sigma^2(V) = \sigma^2(V_0)\left(1 + \frac{V_xV_y + V_xV_z + V_yV_z}{V^2}\right). \quad [11A]$$

Multiplying and dividing the right-hand side by 2 and writing the constant 1 as $(V_x^2 + V_y^2 + V_z^2)/V^2$, Eq. [11A] can be written as Eq. [9] in the text.

ACKNOWLEDGMENT

This work was supported by Grant T32 CA09630-03 from the National Cancer Institute.

REFERENCES

1. C. L. DUMOULIN, S. P. SOUZA, AND H. FENG, *Magn. Reson. Med.* **5,** 47 (1987).
2. T. E. CONTURO, R. R. PRICE, A. H. BETH, D. R. PICKENS, C. L. PARTAIN, AND A. E. JAMES, "Soc. Magn. Reson. Med., Book of Abstracts, New York, 1987," p. 25.
3. T. E. CONTURO, Ph.D. dissertation, Vanderbilt University, Nashville, Tennessee, 1989.
4. T. E. CONTURO AND G. D. SMITH, *Magn. Reson. Med.* **15,** 420–437 (1990).
5. D. LEBIHAN, E. BRETON, D. LALLEMAND, P. GRENIER, E. CABANIS, AND M. LAVAL-JEANTET, *Radiology* **161,** 401–407 (1986).
6. I. R. YOUNG AND G. M. BYDDER, *Radiology* **165(P),** 364 (1987). [Abstract]
7. N. J. PELC, L. R. PELC, R. J. HERFKENS, AND G. H. GLOVER, *Radiology* **177(P),** 171 (1990). [Abstract]
8. N. J. PELC AND M. A. BERNSTEIN, "Soc. Magn. Reson. Med., Book of Abstracts, New York, 1990," p. 475.
9. R. M. HENKELMAN, M. J. BRONSKILL, AND P. R. GOEBEL, *Proc. Soc. Photo-Opt. Instrum. Eng.* **486,** 192 (1984).

10. A. CONSTANTINESCO, C. LALLOT, J. MALLET, A. BONMARTIN, AND P. CARLIER, "Soc. Magn. Reson. Med., Book of Abstracts, New York, 1984," p. 169.
11. M. SPRENGER, *personal communication.*
12. N. J. PELC AND M. A. BERNSTEIN, *Radiology* **177(P),** 171 (1990). [Abstract]
13. T. E. CONTURO AND B. H. ROBINSON, *Magn. Reson. Med.,* submitted for publication.
14. T. E. CONTURO AND B. H. ROBINSON, "Soc. Magn. Reson. Med., Book of Abstracts, San Francisco, 1991," p. 813.
15. P. R. MORAN, *Magn. Reson. Imaging* **1,** 197–203 (1982).
16. V. J. WEDEEN, B. R. ROSEN, R. BUXTON, AND T. J. BRADY, *Magn. Reson. Med.* **3,** 226–241 (1986).
17. H. HOTELLING, *Ann. Math. Stat.* **15,** 297–306 (1944).